IEEE Access
Multidisciplinary | Rapid Review | Open Access Journal

Received October 17, 2018, accepted November 2, 2018, date of publication November 13, 2018,
date of current version December 18, 2018.

Digital Object Identifier 10.1109/ACCESS.2018.2881101

Full Physics Simulation Study of Guardrail Radar-Returns for 77 GHz Automotive Radar Systems

USHEMADZORO CHIPENGO, (Member, IEEE)
ANSYS, Inc., Ann Arbor, MI 48108, USA
e-mail: ushe.chipengo@ansys.com

ABSTRACT Radar is one of the primary active safety sensors for advanced driver assistance systems. Autonomous vehicles will heavily rely on the ability of automotive radar systems to accurately identify crucial targets while filtering out false targets. Road guardrails present a unique corner case challenge to automotive radar sensors due to their large radar cross section (RCS) that can lead to false targets alerts. This paper presents a full physics, full-scale electromagnetic simulation-based study on the radar returns of road guardrails. Results from this paper demonstrate how guardrails can obfuscate crucial targets, such as pedestrians and nearby stationary vehicles. A novel guardrail system for high-pedestrian density areas is proposed. Further RCS reduction of this design is achieved through a proposed diffraction mitigation technique. Simulations using this proposed guardrail system predict over 25-dB reduction in guardrail RCS. Results from this paper show that guardrails with low RCS improve the visibility of adjacent stationary targets, and thus have the potential to reduce accidents and possibly save lives.

INDEX TERMS Automotive radar, radar antenna, simulation, radar cross section.

I. INTRODUCTION

The vision for fully autonomous vehicles equipped with active safety and comfort systems is fast becoming a reality due to the recent rapid developments in advanced driver assistance systems (ADAS). While fully autonomous vehicles are the ultimate goal, an even more pressing requirement has been the need to make roads safer by equipping vehicles with active/passive safety/comfort systems that relieve the driver of any fatigue inducing driving routines while providing crucial situational information.

According to surveys, approximately 90% of accidents are due to human error [1]. Car accidents and their associated costs account to almost 3% of the world's gross domestic product in expenditure [1]. In addition, over 1.25 million people lost their lives worldwide in 2016 to car accidents [2]. In 2010, the United Nations General Assembly declared the years 2011 to 2020 as the *Decade of Action for Road Safety*. To make roads safer, today's vehicles are equipped with advanced driver assistance systems that can provide crucial safety information such as vehicles in the driver's blind spot. In some cases, such as in the automatic emergency braking system (AEB), the vehicle is able to control itself to avoid a collision. Fig. 1 shows some of the advanced driver assistance systems that are available in today's vehicles.

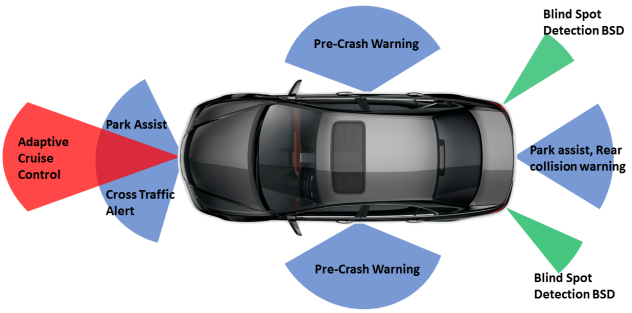

FIGURE 1. Advanced driver assistance systems (ADAS) for active/passive safety/comfort functionality in today's vehicles.

In order for vehicles to have the capabilities shown in Fig.1, they should have an awareness of their position, bearing and velocity in relation to other actors in a traffic scene. Specifically, vehicles must be able to map the distance, velocity and angle of arrival of multiple targets in a highly dynamic environment. Light detection and ranging (Lidar), optical cameras [3]–[6], radio detection and ranging (Radar) and ultrasonic sensors are some of the technologies that are employed to equip vehicles with highly accurate

situational awareness. While the car of the future will routinely fuse data from all these sensors, radar has emerged as the primary sensor technology in active safety/comfort systems. This is because radar is a robust and relatively inexpensive technology that can simultaneously provide the range, velocity and angle of arrival of multiple targets under poor lighting and inclement weather conditions [7]. Automotive radar finds application in adaptive cruise control (ACC), blind spot detection (BSD), rear and front cross traffic alert (CTA), pre-crash warning and automatic emergency braking (AEB) systems.

While radar is a mature technology, it's application in fully autonomous vehicles demands rigorous and extensive testing and validation. Specifically, as radar evolves from merely assisting drivers to passing on sensor information that is used to autonomously control vehicles, stricter reliability constraints will be placed on automotive radar systems. It has been estimated that around 8.8 billion miles [8] of testing will need to be completed before fully autonomous vehicles and their associated sensors are deemed safe for mainstream deployment. To test radar systems, companies and researchers routinely build and test radar systems in live traffic scenarios [7], [9]–[13]. However, this is an expensive, time consuming and impractical approach. Simulation of radar traffic scenes is the only practical way of meeting the rigorous testing demands and demonstrating the reliability of automotive radar systems. Furthermore, using simulation, automotive radar corner cases can be investigated at no risk to automotive companies. Specifically, there are particular scenarios that exist outside of normal operational conditions that can prove fatal for test engineers or future passengers and drivers if not accounted for in radar system design.

An interesting corner case is the impact of road guardrails on radar returns. Guardrails can present themselves to automotive radar systems as high radar cross section targets due to the prevailing dihedral shape of guardrail posts. Dihedrals possess large back-scattering radar cross sections over wide observation angles [14]. Strong radar returns from targets outside the area of interest can confuse radar sensors and lead to either false target identification or failure to detect targets near the guardrail.

Adaptive cruise control (ACC) and automatic emergency braking systems are particularly vulnerable to false targets as they can suddenly slow down a vehicle and potentially cause a rear end collision [1]. For example, Acura recalled 48 000 vehicles due to a faulty emergency braking system caused by radar systems malfunctioning when the vehicle ahead accelerated next to a guardrail or fence. In addition, the National Highway Traffic Safety Administration (NHTSA) investigated instances of Jeep Grand Cherokees unexpectedly engaging the automatic emergency system [15].

Sensor fusion (camera and radar) and probabilistic tracking algorithms have been used to detect guardrails [15]–[17]. However, the success rate of guardrail detection varied in [16], depending on the traffic scene. Furthermore, probabilistic tracking algorithms do not use full physics approaches to model the guardrails. As will be shown in this paper, full physics simulations reveal the distributed nature of radar scene targets while providing insight into other electromagnetic phenomena that simply cannot be picked up by probabilistic approaches.

Both sensor fusion and probabilistic algorithms depend on radar returns to filter out guardrails. Simulation, therefore, is the only practical way of rapidly determining the radar returns of different guardrail designs for sensor fusion and probabilistic algorithm development. Furthermore, cameras and Lidar sensors are affected significantly by visibility and inclement weather, respectively [18]. On the other hand, radar is not significantly affected by visibility and inclement weather, therefore, there can be operating conditions where radar is the only reliable sensor thus making sensor fusion impossible. With this in mind, it is crucial for the radar system of an autonomous vehicle to be extremely reliable.

Full-physics based, electromagnetics simulations of radar traffic scenes have traditionally been highly inefficient due to the large electrical size of radar scenes. Specifically, a typical, full-scale traffic scene is hundreds of billions of cubic wavelengths in size at 77 GHz. While other electromagnetics simulation solvers can model antennas and their associated placement and packaging effects, they cannot carry out a full-physics, electromagnetics analysis of full size radar scenes. Currently, radar scene simulations are conducted on a system level where the targets are considered as point scatterers or reflection models. Such approaches are not full-physics based and neglect the distributed nature of scatterers while failing to capture crucial electromagnetic responses of various targets [19]–[21]. In this paper, the impact of road guardrails on radar returns is investigated using ANSYS' high frequency structure simulator shooting and bouncing ray solver (HFSS SBR+). HFSS SBR+ is a high frequency, asymptotic ray tracing electromagnetic solver that uses physical optics to efficiently solve electrically large problems. Here, HFSS SBR+ was used because of its unique capability to carry out a full-physics electromagnetic analysis of a radar scene while including all electromagnetic transmission, reflection, refraction and diffraction effects.

This paper is organized as follows: Section II focuses on some radar basics and simulation set up. Section III shows the radar returns of a full scale traffic scene with and without guardrails. In section IV, a novel guardrail design is presented. This design has over 25 dB reduction in RCS when compared to conventional guardrails. Here, the Doppler-range maps of the novel and conventional guardrail system designs are compared. Results from simulation show that such a guardrail design can be deployed in regions that have a large traffic/pedestrian density to ensure that the radar system can filter out guardrails in an otherwise complex environment.

This paper has two main contributions, first, it is a full physics based simulation study of road guardrails and their impact on automotive radar returns. Secondly, this work proposes a novel guardrail system that exhibits low RCS along with a radar signature that can be easily filtered.

Such characteristics can aid in easier guardrail and stationary target identification. Accurate guardrail detection can help in preventing accidents and possibly saving lives.

II. TRAFFIC SCENE SIMULATION SETUP IN HFSS SBR+

A. RADAR BASICS

Radar systems emit short bursts of electromagnetic waves and listen for the time delayed, reflected waves that may have encountered an obstacle. For a monostatic radar, the reflected signal power P_r for a target d meters away can be obtained using the radar range equation [22].

$$P_r = \frac{P_t G_t G_r \lambda^2 \sigma_{RCS}}{(4\pi)^3 d^4} \tag{1}$$

Here $P_t, G_t, G_r, \sigma_{RCS}$ and λ represent the peak transmitted power, transmit antenna gain, receive antenna gain, target radar cross section and free space wavelength of the emitted signal. As mentioned previously, guardrails have large radar returns due to the corner reflector shape of the guardrail posts. The maximum RCS of a perfectly conducting dihedral post is given by [23]

$$\sigma_{RCSmax} = \frac{8\pi w^2 h^2}{\lambda^2} \tag{2}$$

Here w and h represent the width and height of the two orthogonal faces, respectively.

While the implementation of various radar systems may vary, radar systems typically seek to simultaneously determine the range, velocity and direction of arrival of multiple targets [13], [24], [25]. Pulsed continuous continuous wave, frequency modulated continuous wave (FMCW), stepped frequency continuous wave (SFCW) and orthogonal frequency division multiplexing are some of the popular variations of radar system implementation [26]. In this paper, HFSS SBR+ will be used to implement a frequency-modulated interrupted continuous-wave radar scheme (FMiCW).

B. SIMULATION SETUP

The traffic scene and its various actors was designed in HFSS SBR+. Fig. 2 shows a full size traffic scene that was modelled in HFSS SBR+ along with the associated range and velocity of each of the targets. Vehicle bodies were assigned as perfect electrical conductors while the road was modelled as a layered impedance asphalt surface. Pedestrians were modelled using the single material dry skin model [27], [28]. Here, the relative dielectric constant and conductivity are $\epsilon_r = 6.6$ and $\sigma = 38.38$ S/m, respectively. The transmit and receive antennas are tapered, series-fed microstrip patch antenna arrays [29], [30] that were designed and optimized at 77 GHz using HFSS FEM solver. Fig. 3 shows the transmit and receive antennas and their associated far field radiation patterns. A summary of the radar simulation parameters is shown in Table.1

III. SIMULATION RESULTS

A radar system can be viewed as an antenna coupling problem in the presence of a scatterer. Specifically, HFSS SBR+ analyzes a radar traffic scene by interrogating the scene and its

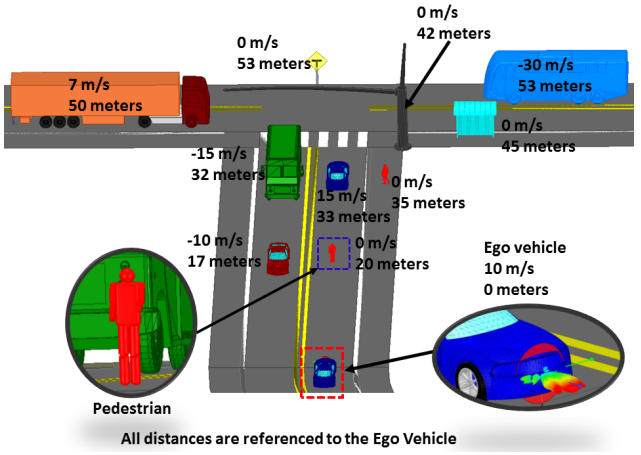

FIGURE 2. Full size (1:1 scale) traffic scene that will be analyzed using HFSS SBR+. The target of particular interest is the pedestrian who is 20 meters ahead of the ego vehicle.

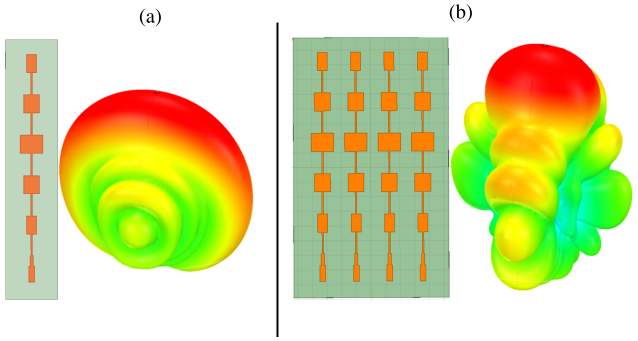

FIGURE 3. Design and far field radiation patterns of the a) Transmit and b) Receive antennas. These antennas are series-fed, microstrip patch antenna arrays that were designed and optimized at 77 GHz using HFSS FEM solver.

TABLE 1. Radar Parameters For Simulation Setup

Parameter	Value
Center Frequency	77 GHz
Start Frequency	76.85 GHz
Stop Frequency	77.15 GHz
Bandwidth	300 MHz
Range Resolution	0.5m
Velocity Resolution	1 m/s
PRF	41.07 kHz
Pulse Width	3.3ns
Number of Pulses	80
Velocity Period	80 m/s

actors using an up-ramp chirp signal. This means that in each pulse, the frequency of the signal is increased from 76.85 GHz to 77.15 GHz. After transmitting the pulse, the transmit antenna is turned off while the receive antenna samples the scattered signal. This scattered signal is weighted by the

radiation pattern of the receive antenna. Using the real and imaginary scattered S parameters, range plots and Doppler-range maps can be obtained with HFSS SBR+. Specifically, an inverse fast Fourier transform (IFFT) of the scattered S parameters is carried out to obtain time domain data that can be easily converted into a range profile since the speed of the signal, c, in free space is known. A Doppler-range map can be constructed by loading multiple range profiles into a radar data matrix and carrying out a fast Fourier transform (FFT) along the columns. The frequency and time domain representations of linear frequency modulated (LFM) pulse waveforms and their associated equations are shown in [31].

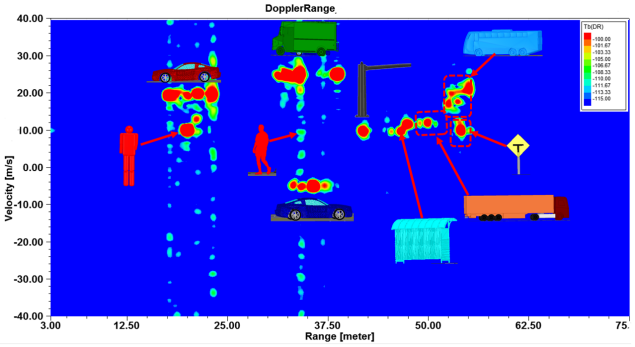

FIGURE 4. Doppler-range map of the radar traffic scene shown in Fig. 2 with the various actors and scene targets superimposed for easier identification. Full physics simulations show that a target is actually a range distributed scatterer as opposed to a point scatterer.

A. OPEN SCENE WITHOUT GUARDRAILS

Fig. 4 shows the Doppler-range map for the traffic scene shown in Fig. 2 with the various actors superimposed on the radar returns for easier identification. It is important to note that this Doppler-range map was obtained using a full physics approach. This means that the propagation, refraction and reflection of electromagnetic waves that make up the FMiCW signal are fully simulated here. This full-physics approach can be seen in the nature of the range distributed radar returns of various targets in the traffic scene. Specifically, a full physics simulation shows that traffic scene actors cannot be considered as point scatterers. Since the ego vehicle is travelling at 10 m/s, all the stationary targets show a relative velocity of 10 m/s. The truck and bus were recorded as having velocities lower than their actual velocities because they are travelling in the direction perpendicular to the ego vehicle.

B. GUARDRAIL CONFINED RADAR SCENE

To investigate the impact of guardrails on radar returns, full size, corrugated w-beam guardrails were placed on both sides of the road shown in Fig. 2. The dimensions, spacing and geometry of the guardrails are to NHTSA specifications. Fig. 5 shows the Doppler-range map of the scene in Fig. 2 when guardrails are placed on either side of the road. This Doppler-range map should be compared to Fig. 4. Note that both Doppler-range maps use the same intensity

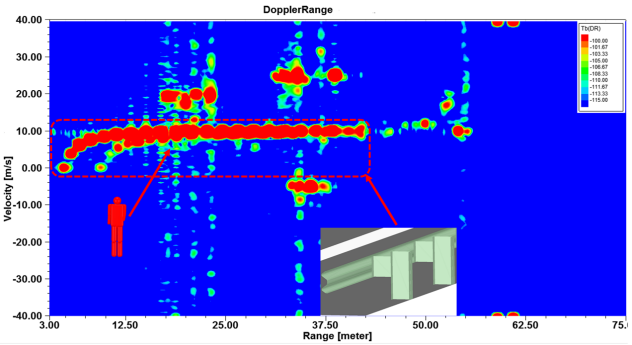

FIGURE 5. Doppler-range map of the radar traffic scene shown in Fig. 2 with guardrails on either side of the road. Guardrails provide strong returns that resemble multiple stationary targets. Comparing Fig. 4 and Fig. 5 shows how the pedestrian radar returns are overwhelmed by guardrails.

scale for a direct comparison. From Fig. 5, it can be seen that guardrails present themselves as extremely strong stationary targets. Of even greater significance is how guardrail returns are overwhelming pedestrian radar returns. Such a result shows that crucial stationary targets near guardrails can be obfuscated by the strong radar returns of guardrails. Specifically, in order for autonomous vehicles to operate based on radar returns, they need to be able to filter out certain radar returns belonging to targets such as guardrails while simultaneously tracking targets of interests such as pedestrians and vehicles. Guardrails complicate this process by presenting the radar system with multiple stationary targets that have strong radar returns. During guardrail filtering, a radar system can possibly, by mistake, ignore a pedestrian standing next to the guardrails.

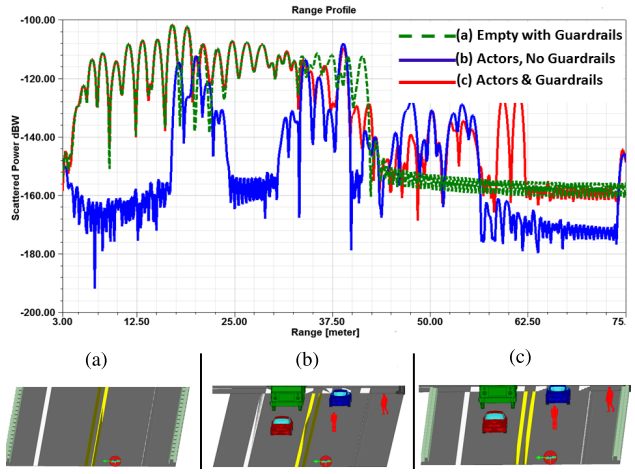

FIGURE 6. Range profile for different road scenarios a) Empty road with no actors b) Road with actors but no guardrails as shown in Fig. 2 c) Road with actors and guardrails. Observe how guardrails dominate the range profile of the entire scene.

Another way to see how guardrails saturate traffic scene radar returns is to look at single range profiles. Fig. 6 shows a range profile for three different instances. In the first case, an empty, guardrail confined road with no actors is interrogated. In the second case, the guardrails are removed and

replaced with the same scene as in Fig. 2. Finally, a scene with both guardrails and actors is also interrogated. It can be seen that the guardrail radar returns dominate the overall characteristics of the range profile. As already noted, this is because guardrails posts are shaped like dihedral corner reflectors. The w-beam corrugated shape of the rails also enhances the guardrail RCS.

IV. A NOVEL LOW RCS GUARDRAIL SYSTEM FOR HIGH TRAFFIC DENSITY AREAS

A. GEOMETRY AND MATERIAL-BASED RCS REDUCTION TECHNIQUES

A mature technique of reducing the RCS of targets especially in military applications is to coat them in materials that act as either passive or active radar absorbers [14]. Conventional radar absorbers reduce the intensity of the reflected signal through destructive interference and/or by absorbing the incident electromagnetic energy and converting it into into heat [32]. Active absorbers such as the phase-switched-screen PSS reduce the RCS by modulating the interrogating incident signal and redistributing its energy over a wide bandwidth typically into the sidebands of the radar receiver. As a result of this, a very small amount of reflected energy will be within the bandwidth of the receiver, thus making the target virtually invisible [33], [34]. Even more interesting radar deception techniques can be achieved using the PSS to generate multiple targets with almost identical range profiles at different locations [35], [36]. Although effective in other applications, passive and active absorbers may not be well suited for application in road infrastructure due to cost, practicality of implementation and reliability. Specifically, to use passive absorbers, guardrails would need to be coated by 2 to 3 inches of the absorbing material to avoid reflections from the backing guardrail metal [32]. Furthermore, at 77 GHz, absorbers are extremely sensitive to material depth, deformation, adhesive or paint layers, transition gradient of loaded materials and inhomogeneity of material properties [32]. Another issue is the durability of the absorbers and their ability to withstand multiple weather season cycles. Active absorbers such as the PSS are expensive to implement in road infrastructure that will need to be deployed on a large scale. Furthermore, a PSS based guardrail system will require highly reliable and robust electronic components to prevent any possible system malfunction over a long period of time. On the other hand, a geometry based RCS reduction approach will not require any costly material or electronics additions to the existing infrastructure. Furthermore, the materials used in today's guardrails are highly reliable and resistant to weather effects. For these reasons, this paper will focus only on geometry based RCS reduction techniques.

B. PROPOSED GUARDRAIL WITH GEOMETRY-BASED RCS REDUCTION

In the previous section, the large RCS of road guardrails was investigated and shown to have the ability to potentially mask the presence of crucial, low velocity targets in the guardrail's proximity. This can be dangerous in high traffic/pedestrian density areas. In this section, a novel guardrail system with a low RCS is proposed for such areas. Low RCS guardrails make it easier for automotive radar systems to filter them out during operation. Here, the guardrail design is based on the w-beam corrugated guardrail that was already presented. In order to reduce the guardrail post RCS, a flat metallic sheet was put in place of the w-beam to entirely cover the posts. This is because w-beam rails also exhibit some dihedral scattering characteristics. However, a flat sheet is not a good back-scatterer at oblique angles of incidence. It is important to note that the rest of the guardrail posts dimensions such as height remained unchanged to adhere to NHTSA's standards.

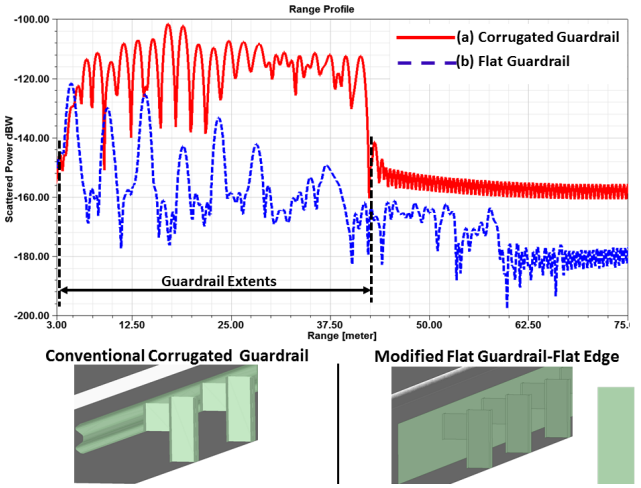

FIGURE 7. Range profiles for empty roads with a) The conventional w-beam corrugated guardrail b) Flat sheet guardrail system. The proposed guardrail system has a lower RCS than a conventional guardrail system.

To investigate the impact of this design, a 42.5m long section of the novel guardrail system was simulated using HFSS SBR+. Fig. 7 shows the proposed guardrail design and range profiles of both the conventional w-beam guardrail and the proposed flat sheet guardrail system. As seen in Fig. 7, the proposed guardrail system lowers the RCS by over 25 dB. The goal is to design a guardrail system that does not have a large enough RCS to overwhelm radar sensors in areas with multiple low velocity actors such as pedestrians.

C. REDUCTION OF PROPOSED GUARDRAIL SYSTEM RCS THROUGH EDGE DIFFRACTION MITIGATION

Although the proposed guardrail system shown in Fig. 7 has a much lower RCS, the radar returns of this proposed guardrail are not consistent with its length. Specifically, the proposed guardrail system has relatively prominent radar returns between 42.5m and 60m. On the other hand, the radar returns of the conventional guardrail system are consistent with its length as shown in Fig.7. This can be explained using the theory of edge diffraction [37]. Specifically, the edges of the flat metal plate create current discontinuities that lead to diffraction [38]. It is these diffracted rays that are reflected

back onto the opposite flat plate before they are finally captured by the receive antenna of the radar system. Rays that experience multiple bounces before returning to the radar sensor can represent a larger range due to their increased path length. While diffraction still occurs on the w-beam guardrail edges, the orientation of the diffraction edge favors scattering in the direction away from the reflecting walls. Furthermore, the curvature of the w-beam guardrail destructively distorts the reflection phase fronts of any diffraction rays incident on it.

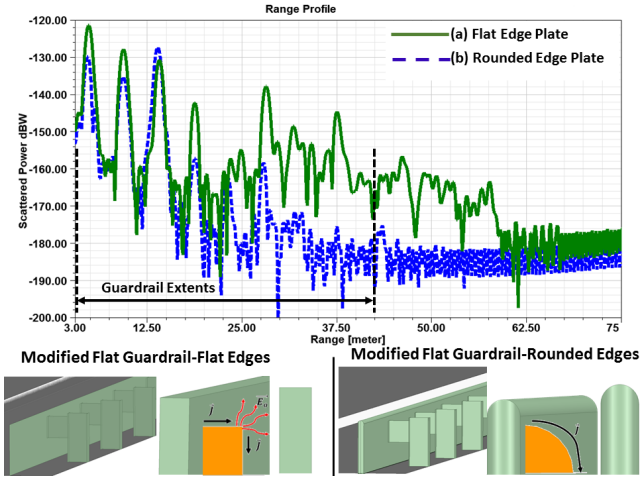

FIGURE 8. Range profiles for empty roads with a) The proposed guardrail plate with flat edges b) The proposed guardrail plate with rounded edges. Rounding the plate edges reduces the current *J* discontinuity and thus reduces the overall radar returns of the proposed guardrail system.

One way of reducing diffraction is to reduce the current discontinuity at the plate edges by rounding the flat plate edges. Fig. 8 shows the proposed guardrail system with flat and rounded edges. As predicted, the radar returns of the rounded edge plate decay consistently with the physical extents of the guardrail. To demonstrate the effectiveness of the diffraction reduction technique applied here, an empty road, 42.5m long was fitted with the conventional w-beam guardrails and the proposed guardrail system with rounded edges. Fig. 9 shows a comparison of the range profiles of these two scenarios. Here, the radar returns of the proposed guardrail system are consistent with its physical length due to a reduction of the edge diffraction effects. It should be noted that the setup for the simulation in Fig.9 is identical to the one used in Fig. 7 except for the now rounded plate edges.

D. INVESTIGATING THE EFFECTIVENESS OF THE PROPOSED GUARDRAIL SYSTEM IN FULL TRAFFIC SCENES

To investigate the effectiveness of the proposed guardrail system, a scene identical to Fig. 2 was fitted with the proposed guardrail system. Fig. 10 shows range profiles of the scene in Fig. 2 and the same scene fitted with the proposed guardrail system. Of interest is how the range profiles more closely follow each other as compared to the case shown in Fig. 6.

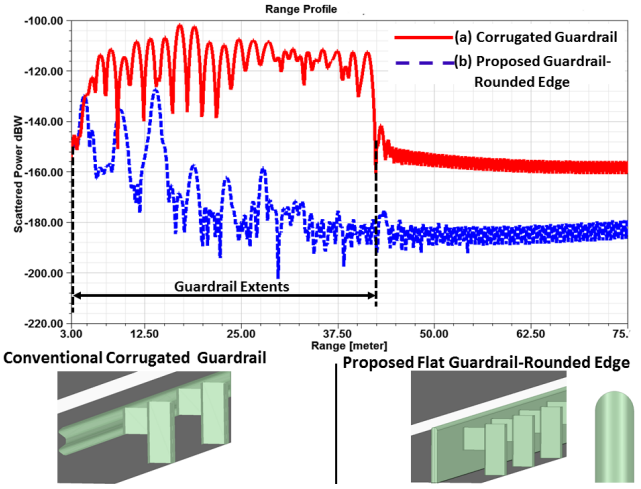

FIGURE 9. Range profiles for empty roads with a) The conventional w-beam corrugated guardrail b) Flat sheet guardrail system with rounded edges for diffraction mitigation. Mitigating diffraction effects makes the radar returns of the proposed guardrail system consistent with its physical extents.

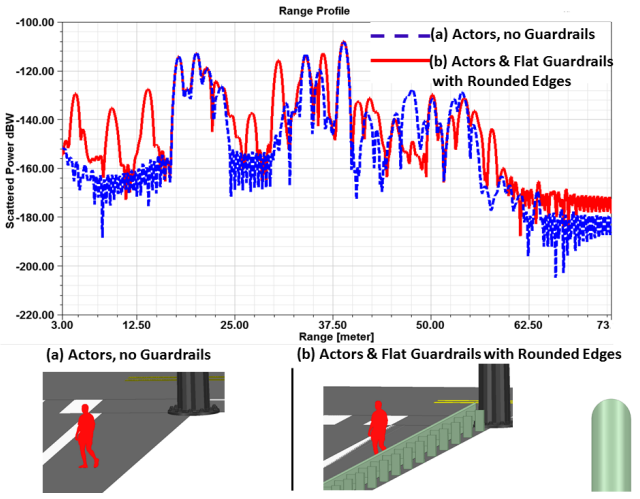

FIGURE 10. Range profiles for the full traffic scene shown in Fig. 2 a) Without guardrails b) With the proposed guardrail system with diffraction mitigating rounded edges. The proposed guardrail system does not overwhelm the radar returns of other actors in the scene.

Here, the guardrails are not overwhelming the radar returns of the various actors in the scene. A lower guardrail RCS is extremely important as it makes it easier for the radar system to identify pedestrians standing next to the guardrail. Fig. 11 shows the Doppler-range map of the scene shown in Fig. 2 when the proposed guardrails are installed before diffraction mitigation. As predicted, when compared to the conventional guardrail system (see Fig. 5), the proposed guardrail system has a much lower RCS as evidenced by the reduced radar returns. Here, the stationary pedestrian can now be seen at a range of 20 meters with a relative velocity of 10 m/s.

Although the proposed guardrail system shown in Fig. 10 and Fig. 11 does not overwhelm the radar returns

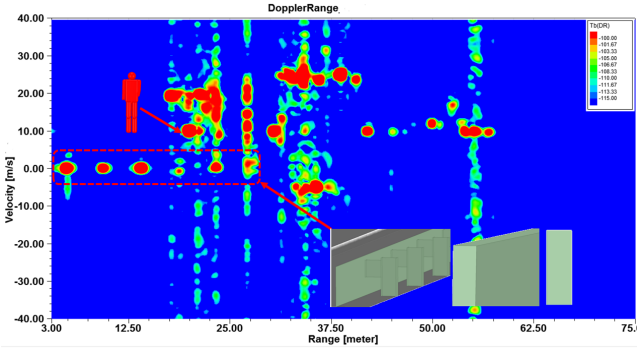

FIGURE 11. Doppler-range map of the traffic scene shown in Fig. 2 when fitted with the proposed guardrail system *before diffraction mitigation*.

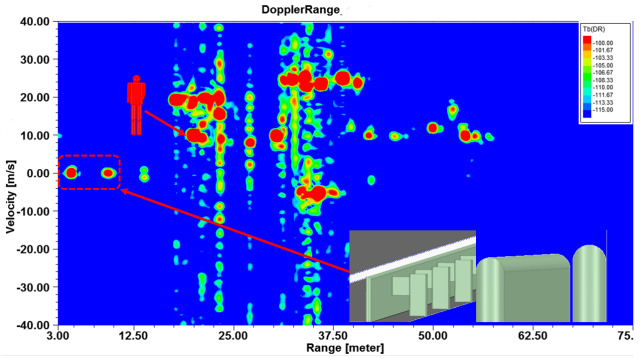

FIGURE 12. Doppler-range map of the traffic scene shown in Fig. 2 when fitted with the proposed guardrail system *after diffraction mitigation*.This should be compared to the Doppler-range map of the conventional w-beam corrugated guardrail shown in Fig. 5.

of other actors in the scene, it also introduces its own radar returns. Specifically, there are strong returns observed between the 3m and 28m range. The first two peaks correspond to the radar returns of the guardrail plate immediately to the sides of the ego vehicle. Here, rays from the transmit antenna have normal incidence to the metallic plates. The reflected rays are captured by the receive antenna sidelobes and thus present strong returns due to their proximity. The remaining radar return peaks from 10m to 28m cannot be simply explained using Snell's law of reflection. This is because Snell's law predicts that the incident rays would be reflected forward at an angle equal to the angle of incidence due to the guardrail's flat geometry. However, the additional peaks can be explained using both Snell's law of reflection and the theory of edge diffraction [37]. Specifically, edge diffracted rays at the edges of the guardrails backscatter to the receive antenna either via direct paths or single bounce paths. To demonstrate this, another simulation of the proposed guardrail system with diffraction mitigating rounded edges was carried out. Fig. 12 shows the Doppler-range map for the scene shown in Fig. 2 with the diffraction mitigated proposed guardrail system. By comparing Fig. 11 and Fig. 12, it can be seen that almost all the peaks corresponding to the proposed guardrail system between 10m and 28m disappear when the diffraction effects are mitigated. The remaining peaks are due to the side reflection of the guardrail system. By comparing Fig. 12 and Fig. 5, it can be seen that the remaining two peaks of the proposed guardrail system in Fig. 12 are much easier to filter out of the Doppler-range map than those in Fig. 5.

A salient feature of the proposed guardrail system is the almost 0 m/s relative radial velocity that it presents to the ego vehicle travelling at 10 m/s as seen in Fig. 12. This means that the guardrail system seems to be travelling at 10 m/s as well. This can be explained by considering that radar measures the radial velocity, therefore, a high velocity perpendicular to the ego vehicle can be perceived as a low radial velocity. In this case, the proposed guardrail system exhibits an almost 0 m/s radial velocity because of its low back-scattering geometry at oblique incidence. Only the portion of the guardrails next to the ego vehicle back-scatter significant radar returns at near normal incidence angles. Such Doppler-range characteristics of the proposed design can be exploited to make it even easier to filter out the guardrail system. This should be compared to the dihedral posts in the conventional guardrail system (see Fig. 5) that exhibit a larger back-scatter RCS and thus a greater radial velocity (equal to that of stationary targets) to the radar system.

V. CONCLUSION

Radar is the primary sensor technology for active safety and advanced driver assistance systems because it can simultaneously determine the range, velocity and direction of arrival of multiple targets without being adversely affected by inclement weather and low visibility. Before radar systems are deployed in fully autonomous vehicles, they need to be extensively tested for reliability. Simulation has emerged as the most practical way of investigating automotive radar corner cases. In this paper, HFSS SBR+ full physics based simulations were used to investigate the high radar returns of road guardrails. Results from this study showed how guardrails can obfuscate low velocity targets such as a pedestrian 20 meters away from the ego vehicle. Using insight from this study, a novel, low RCS guardrail system for high traffic/pedestrian density areas was proposed. Further RCS reduction of this proposed guardrail system was achieved by rounding the plate edges to reduce current discontinuity. Simulations showed a reduction in radar returns by over 25 dB. Low RCS guardrails allow for easier filtering of guardrail systems while improving the visibility of critical targets such as pedestrians standing next to guardrails.

ACKNOWLEDGMENT

The authors would like to thank C. Matara and S. Carpenter for their constructive ideas and contributions during the development of this work.

REFERENCES

[1] A. K. Yadav and J. Szpytko, "Safety problems in vehicles with adaptive cruise control system," *J. KONBiN*, vol. 42, no. 1, pp. 389–398, 2017.

[2] R. Sagar, "Making cars safer through technology innovation," Texas Instrum., Dallas, TX, USA, Tech. Rep., 2017, pp. 1–10. [Online]. Available: http://www.ti.com/lit/wp/sszy009a/sszy009a.pdf

[3] R. H. Rasshofer and K. Gresser, "Automotive radar and lidar systems for next generation driver assistance functions," *Adv. Radio Sci.*, vol. 3, pp. 205–209, May 2005.
[4] D. M. Gavrila, "The visual analysis of human movement: A survey," *Comput. Vis. Image Understand.*, vol. 73, no. 1, 82–98, 1999.
[5] T. B. Moeslund, A. Hilton, V. Krüger, "A survey of advances in vision-based human motion capture and analysis," *Comput. Vis. Image Understand.*, vol. 104, nos. 2–3, pp. 90–126, 2006.
[6] R. Poppe, "Vision-based human motion analysis: An overview," *Comput. Vis. Image Understand.*, vol. 108, nos. 1–2, pp. 4–18, 2007.
[7] G. Reina, D. Johnson, and J. Underwood, "Radar sensing for intelligent vehicles in urban environments," *Sensors*, vol. 15, no. 6, pp. 14661–14678, 2015.
[8] Forbes. (Oct. 2016). *Toyota's Robot-Car Line in the Sand: 8.8 Billion Test Miles to Ensure Safety*. [Online]. Available: https://www.forbes.com/sites/alanohnsman/2016/10/03/toyotas-robot-car-line-in-the-sand-8-8-billion-test-miles-to-ensure-safety/#7ec9a12316f0
[9] J. Hasch, R. Topak, T. Schnabel, T. Zwick, R. Weigel, and C. Waldschmidt, "Millimeter-wave technology for automotive radar sensors in the 77 GHz frequency band," *IEEE Trans. Microw. Theory Techn.*, vol. 60, no. 3, pp. 845–859, Mar. 2012.
[10] K. Ohguchi, M. Shono, and M. Kishida, "79 GHz band ultra-wideband automotive radar," *Fujitsu Ten Tech. J.*, vol. 39, pp. 9–14, 2013. [Online]. Available: http://www.denso-ten.com/business/technicaljournal/30_39.html
[11] J. Singh, S. Rao, and R. Ramasubramanian, "AWR1642 mmWave sensor:76-81 GHz radar-on-chip for short range radar applications," Texas Instrum., Dallas, TX, USA, Tech. Rep., 2017, pp. 1–7. [Online]. Available: http://www.ti.com/lit/wp/spyy006/spyy006.pdf
[12] B.-H. Ku *et al.*, "A 77–81-GHz 16-element phased-array receiver with±50° beam scanning for advanced automotive radars," *IEEE Trans. Microw. Theory Techn.*, vol. 62, no. 11, pp. 2823–2831, Nov. 2014.
[13] *Implementing Digital Processing for Automotive Radar Using SoCs*, Altera Corp., San Jose, CA, USA, 2013, 1–15.
[14] E. L. Nohara, M. A. S. Miacci, G. G. Peixoto, I. M. Martin, and M. C. Rezende, "Radar cross section reduction of dihedral and trihedral comer reflectors coated with radar absorbing materials (8–12 GHz)," in *IEEE MTT-S Int. Microw. Symp. Dig.*, Sep. 2003, pp. 479–484.
[15] T. Kim and B. Song, "Detection and tracking of road barrier based on radar and vision sensor fusion," *J. Sensors*, vol. 2016, Aug. 2016, Art. no. 1963450. [Online]. Available: https://www.hindawi.com/journals/js/2016/1963450/cta/
[16] G. Alessandretti, A. Broggi, and P. Cerri, "Vehicle and guard rail detection using radar and vision data fusion," *IEEE Trans. Intell. Transp. Syst.*, vol. 8, no. 1, pp. 95–105, Mar. 2007.
[17] C. Adam, R. Schubert, N. Mattern, and G. Wanielik, "Probabilistic road estimation and lane association using radar detections," in *Proc. 14th Int. Conf. Inf. Fusion*, Chicago, IL, USA, Jul. 2011, pp. 1–8.
[18] R. H. Rasshofer, M. Spies, and H. Spies, "Influences of weather phenomena on automotive laser radar systems," *Adv. Radio Sci.*, vol. 9, pp. 49–60, Jul. 2011.
[19] T. Johansson, A. Andersson, M. Gustafsson, and S. Nilsson, "Positioning of moving non-line-of-sight targets behind a corner," in *Proc. 13th Eur. Radar Conf.*, London, U.K., Oct. 2016, pp. 181–184.
[20] T. Schipper, J. Schlichenmaier, D. Ahbe, T. Mahler, J. Kowalewski, and T. Zwick, "A simulator for multi-user automotive radar scenarios," in *IEEE MTT-S Int. Microw. Symp. Dig.*, Apr. 2015, pp. 1–4.
[21] L. Huang, H. Chen, and J. Bai, "Simulation of the effect of signal source's phase noise on millimeter wave automotive radar system based on SystemVue," in *Proc. IEEE Int. Workshop Electromagn., Appl. Student Innov. Competition (iWEM)*, May 2016, pp. 1–3.
[22] C. A. Balanis, "Fundamental parameters of antennas," in *Antenna Theory: Analysis and Design*. Hoboken, NJ, USA: Wiley, 2013, p. 98.
[23] M. A. S. Miacci, E. L. Nohara, G. G. Peixoto, I. M. Martin, and M. C. Rezende, "Indoor radar cross section measurements of simple targets," *J. Aerosp. Technol. Manage.*, vol. 4, no. 1, pp. 25–32, Mar. 2012.
[24] M. A. Richards, J. A. Scheer, and W. A. Holm, *Principles of Modern Radar: Basic Principles*. Rijeka, Croatia: SCITech, 2010.
[25] C. Iovescu and S. Rao, "The fundamentals of millimeter wave sensors," Texas Instrum., Dallas, TX, USA, Tech. Rep., 2017, pp. 1–8. [Online]. Available: http://www.ti.com/lit/wp/spyy005/spyy005.pdf
[26] S. M. Patole, M. Torlak, D. Wang, and M. Ali, "Automotive radars: A review of signal processing techniques," *IEEE Signal Process. Mag.*, vol. 34, no. 2, pp. 22–35, Mar. 2017.
[27] T. Wu, T. S. Rappaport, and C. M. Collins, "The human body and millimeter-wave wireless communication systems: Interactions and implications," in *Proc. IEEE Int. Conf. Commun. (ICC)*, Jun. 2015, pp. 2423–2429.
[28] D. Belgiovane, C.-C. Chen, M. Chen, S. Y.-P. Chien, and R. Sherony, "77 GHz radar scattering properties of pedestrians," in *Proc. IEEE Radar Conf.*, May 2014, pp. 0735–0738.
[29] T. Yuan, N. Yuan, and L.-W. Li, "A novel series-fed taper antenna array design," *IEEE Antennas Wireless Propag. Lett.*, vol. 7, pp. 362–365, 2008.
[30] Y. I. Chong and D. Wenbin, "Microstrip series fed antenna array for millimeter wave automotive radar applications," in *IEEE MTT-S Int. Microw. Symp. Dig.*, Sep. 2012, pp. 1–3.
[31] N. Tai, L. Gao, X. Xu, M. Li, H. Han, and L. Liu, "Active cancellation method against LFM radar using periodic sequence phase-modulation," in *Proc. 2nd IEEE Adv. Inf. Manage., Communicates, Electron. Autom. Control Conf. (IMCEC)*, May 2018, pp. 536–540.
[32] Z. Chen, "Common RF absorbers evaluations in W-band (75-100 GHz)," in *Proc. IEEE Int. Symp. Electromagn. Compat. Signal/Power Integrity (EMCSI)*, Aug. 2017, pp. 1–31.
[33] B. Chambers and A. Tennant, "A smart radar absorber based on the phase-switched screen," *IEEE Trans. Antennas Propag.*, vol. 53, no. 1, pp. 394–403, Jan. 2005.
[34] B. Chambers and A. Tennant, "Influence of switching-waveform characteristics on the performance of a single-layer-phase switched screen," *IEEE Trans. Electromagn. Compat.*, vol. 44, no. 3, pp. 434–441, Aug. 2002.
[35] L. Xu, D. Feng, R. Zhang, and X. Wang, "High-resolution range profile deception method based on phase-switched screen," *IEEE Antennas Wireless Propag. Lett.*, vol. 15, pp. 1665–1668, 2016.
[36] J. Wang, D. Feng, L. Xu, and W. Hu, "Synthetic aperture radar image modulation using phase-switched screen," *IEEE Antennas Wireless Propag. Lett.*, vol. 17, no. 5, pp. 911–915, May 2018.
[37] P. M. Bakker, "Theory of edge diffraction in terms of dynamic ray tracing," *Geophys. J. Int.*, vol. 102, no. 1, pp. 177–189, 1990.
[38] A. Savin, F. Novy, S. Fintova, and R. Steigmann, "Evaluation of thin discontinuities in planar conducting materials using the diffraction of electromagnetic field," *IOP Conf., Mater. Sci. Eng.*, vol. 227, p. 012115, Aug. 017.

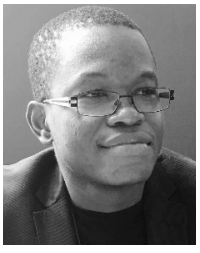

USHE CHIPENGO received the B.S. degree *(summa cum laude)* in electrical engineering from the University of Nicosia, Cyprus, in 2013, and the M.Sc. and Ph.D. degrees in electrical engineering from The Ohio State University in 2017. With a focus on electromagnetics, he has conducted research on slow wave structures for high-power microwave sources, antennas, microwave circuits, and computational electromagnetics.

Since 2017, he has been with ANSYS, Inc., as an Application Engineer II. His current research interests include antenna design for automotive applications and automotive radar for advanced driver assistance systems.